URSI AP-RASC 2019, New Delhi, India; 09 - 15 March 2019

Suspended Metasurface Loaded Dual Band Dual Polarized Dipole Antenna Array with Polarization Flexibility for RF Energy Harvesting

Vinnakota Sarath Sankar(1), Basudev Majumder*(2), Krishnamoorthy K(3) and Runa Kumari(1)
(1) Department of EEE, BITS Pilani Hyderabad Campus, Hyderabad, India, 500078
(2) Department of Avionics, IIST, Thiruvananthapuram, India, 695547
(3) Department of ECE, NIT Surathkal, Mangalore, India, 575 025

Abstract

The paper presents a dual band dual polarized antenna working at frequencies of 2.18 GHz and 2.9 GHz. The antenna has a realized gain of 8.2 dB and 8.78 dB at 2.18 GHz and 2.9 GHz respectively. This is integrated with a energy harvesting circuit through a network consisting of a rat race coupler and a dual frequency wilkinson power divider. The harvesting circuit provides a power conversion efficiency of 68.8 % at 5 dBm input power.

1 Introduction

Metamaterial based antennas are widely used nowadays for various applications. Various types of metamaterials and their applications in designing novel electromagnetic devices have been presented in [1]. Metamaterial antennas have been used for improving the gain of the antennas [2–5]. The high gain antennas find applications in design of energy harvesting rectennas [6].

Energy harvesting is being investigated for low power wireless sensor network applications, mainly to eliminate the use of batteries, thereby reducing the environmental pollution as well as eliminating the need for manual intervention in replacing the used batteries. Due to abundance of RF energy in the environment in the form of cellular base stations, Wi-Fi routers etc., a portion of the radiated energy can be harvested to power up the sensors. Many recent works [7] reported the use of rectennas, a combination of antenna and energy harvesting circuit, for extracting ambient RF energy from the environment. A rectifying circuit with a half wave rectifier topology consists of a schottky diode, a DC low pass filter and load. Stepped impedance filter has been used in [8] as a DC pass filter to suppress the higher harmonics. In [6], a dual band array antenna has been used for harvesting, which also uses a stepped impedance DC pass filter. In [9], a dual band dual polarized antenna is designed where one port was used for transmission and other port for energy harvesting applications with a gain of 7.2 dB.

In this paper, an integrated metasurface loaded dual band dual polarized dipole antenna is designed. Dual polarization is obtained be placing a similar antenna orthogonal to the first antenna. Lower band of the antenna which is operating at GSM 2.2 GHz band is used for RF energy harvesting and the higher operating band is kept for transmitting purpose. The power received from both the antenna is given to a network that separates the two bands of the antenna and harvests energy from a single frequency band.

The paper is divided into following sections. Section 2 gives description about the antenna design. In section 3, rectifying circuit construction is explored briefly. In subsequent sections, the results of the overall network have been presented followed by conclusions drawn.

2 Antenna Design

The antenna design has been shown in Fig. 1. The antenna has been made up using a simple cylindrical dipole having two arms which was extruded from the metallic feed line portion of the Microstrip BALUN. A planar microstrip balanced to unbalanced transmission line is designed to match the antenna from the single ended source. This microstrip BALUN is designed on a substrate having permittivity of 2.2, loss tangent of 0.001and thickness of 0.8 mm. Further to enhance the radiation pattern of the antenna that is to make it unidirectional and to induce a surface wave assisted mode, an optimized AMC based metasurface is designed. Two metasurface based dipole antennas are placed orthogonal to each other as shown in Fig. 1 (b) to achieve polarization diversity as well as good isolation characteristics.

3 Rectifier Circuit Design

The rectifying circuit shown in Fig. 2 is designed two stages. In the first stage, the dual frequency inputs at 2.18 GHz and 2.9 GHz from the antenna are given to the two inputs of the rat race coupler (RRC) [10]. The rat race coupler is designed for a frequency of 2.54 GHz so that it can cover both the bands. The combined signal is collected at the sum port of the coupler. This output signal is given to a dual band wilkinson power divider working effectively at a frequency of 2.18 GHz and 2.9 GHz respectively [11]. The combined signal is then split equally in both the frequency bands. The output power from the branches is further given

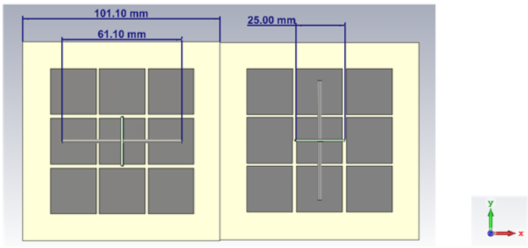

(a) Top view

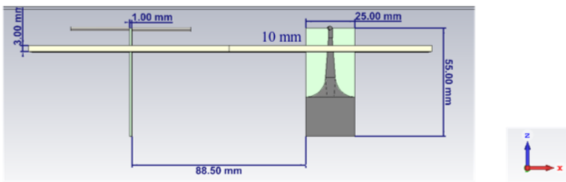

(b) Side view

Figure 1. Geometry of the antenna

to a butterworth band pass filter to pass only the respective frequency component. By this way, the two ports of the dual frequency Wilkinson power divider will have the frequencies of 2.18 GHz and 2.9 GHz respectively. The design has been realized in Keysight ADS [12]. The two inputs to the rat race coupler are two tone power sources, representing the two antennas. In the subsequent stage a

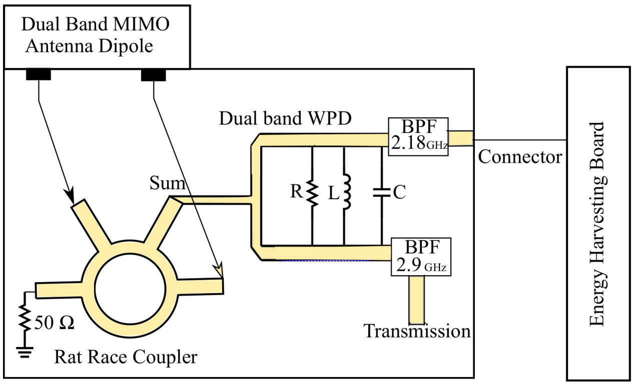

Figure 2. Rat race coupler combined with dual band Wilkinson power divider

energy harvesting circuit shown in Fig. 3 is designed to harvest the energy at 2.18 GHz. The circuit consists of a stepped impedance low pass filter, a load of 1000 Ohms, connected to commercially available schottky diode HSMS 2850 [13]. The impedance of the network is matched to the first stage by means of a open stub matching network, designed and optimized in Keysight ADS [12]. The entire circuit has been designed using ideal transmission lines and can be implemented using microstrip framework for practical applications. The entire circuit has been designed using ideal transmission lines and would be implemented using microstrip transmission lines for future applications.

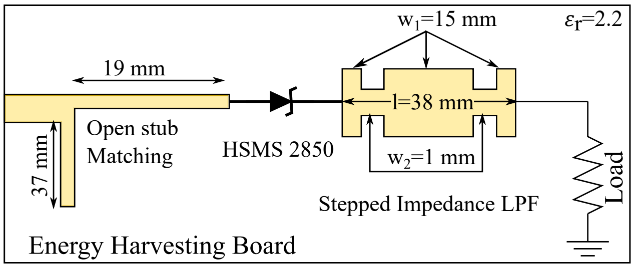

Figure 3. Energy harvesting board

4 Results

4.1 Antenna results

Figure 4 shows the unit cell of the Artificial Magnetic Conductor and its description when it is working in as a Reactive Impedance Surface (RIS). Fig 4 (b) is used to calculate the phase constant over the frequency in CST MWS [14] with proper boundary conditions. This AMC unit cell is printed on Rogers RO3003 substrate having permittivity of 3, loss tangent of 0.001 and thickness of 3mm. Fig. 5 de-

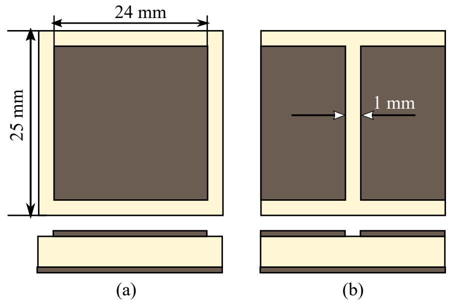

Figure 4. (a) AMC Unit Cell (b) RIS Configuration

picts the characteristics of the proposed patch type AMC surface. From Fig. 5(a) it is noticed that at 2.2 GHz the inductive phase of the reflection phase compensates the capacitive effect of the below dipole resonance which is essential for good input impedance matching. Also due to the near zero reflection phase at around 2.2 GHz the dipole radiation becomes unidirectional and the front to back lobe ratio (FTBR) enhances remarkably. Fig. 5(b) shows the electric field distribution in the YZ plane at 2.2 GHz. It describes that the AMC loaded dipole antenna radiates mainly from the central region of the dipole at the lower resonance. Fig. 5(d) depicts the amplitude of the E filed in the X direction at 2.9 GHz. It is also observed that on the top plane of the metasurface, the tangential component of the Magnetic Field exhibits higher intensity in the Y direction. From these plots it can be inferred that the AMC Surface radiates along the two open ends in the X direction. These plots also show that the higher resonance is obtained due to the TM surface wave coupling along the X direction which was further verified by the TM surface wave dispersion diagram presented in Fig. 5 (c). It shows that a single RIS based (shown in Fig. 4(b)) patch can produce 300 phase shift at around 3.1 GHz (shown by the coordinates in the Fig. 5(c)),

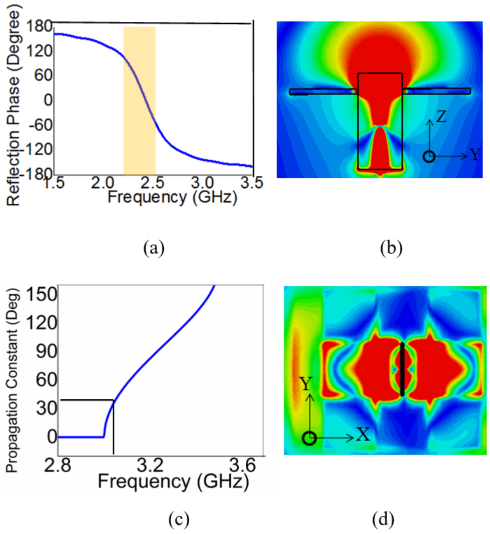

Figure 5. (a) Reflection phase curve over frequency band. (b) Amplitude of the Ex above the metasurface at 2.9 GHz (c) Phase-shift variation over the frequency. (d) Electric field distribution at XZ Plane at 2.9 GHz

So in order to excite TM_{01} (for 180^0 phase shift) three of such unit cells are combined. But because of the presence of the fringing fields from both the open ends along the X direction, the simulated resonating frequency becomes is observed less and it is around 2.9 GHz. This surface wave assisted mode excitation is done parasitically from the dipole antenna. So by this technique a dual band unidirectional antenna can be designed with good gain and high FTBR. It is noticed that at the lower band, antenna FTBR is noted around 17 dB and at the higher band the antenna FTBR is observed around 25 dB. When compared with [9],

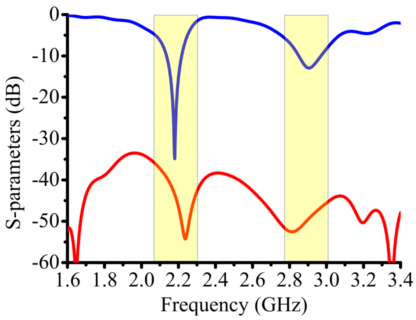

Figure 6. S parameter plot of the antenna S_{11}, S_{12}

the performance of the antenna is increased, both in terms of gain as well as FTBR. The reflection co-efficient plot of the antenna is shown in Fig. 6. The antenna resonates at 2.2 GHz with a return loss of 35 dB and 2.9 GHz with a return loss of 13 dB as indicated by the shaded bands. The radiation patterns of the antennas have been shown in Fig. 7 for both the resonating frequencies. The simulated gains of the antenna are observed around 8.2 dB and 8.78 dB at the frequencies 2.18 GHz and 2.9 GHz, respectively. These are about 5 dB more than that of a conventional dipole antenna gain. The cross polarization level is observed less than -15 dB in both the principal planes of the antenna.

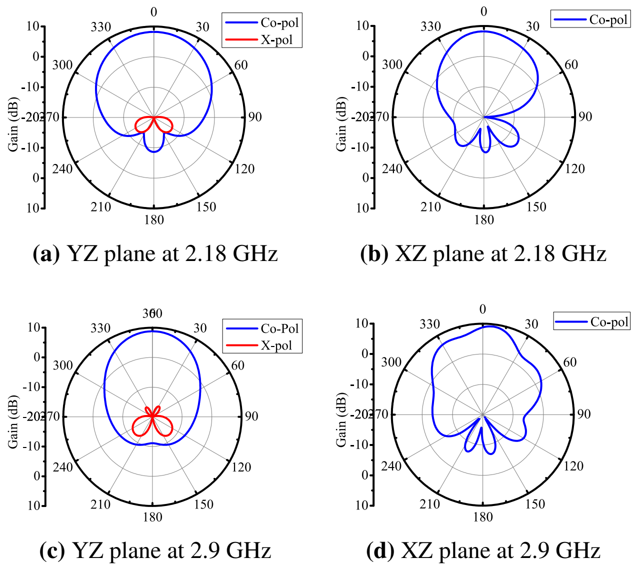

Figure 7. Radiation pattern plots of the antennas at 2.18 GHz and 2.9 GHz

4.2 Rectifier Circuit results

The output power at the sum port of the rat race couple is shown in Fig. 8. The two input power from the antennas at the respective terminals are added up at this terminal and this combination is fed to the dual band WPD. In Fig. 9 the output of the band pass filters at the terminals of the dual band WPD are shown along with the combined inputs. It can be observed that the band pass filters filter out the individual frequency components at 2.18 GHz and 2.9 GHz respectively. The rectifying circuit is designed to operate

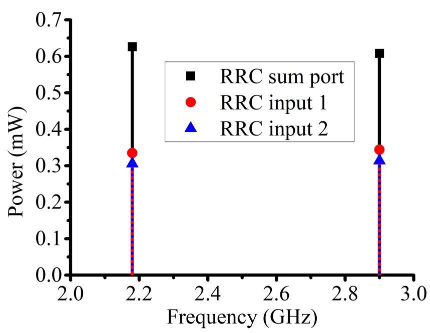

Figure 8. Power at the input and output of Rat Race coupler

at a frequency of 2.18 GHz. The power received by the SMA connector is passed to the load through matching network, diode and the rectifying circuit. The performance of the rectifier circuit is mainly evaluated by the parameter, power conversion efficiency (PCE). The power conversion efficiency is given by the equation:

$$PCE(\%) = \frac{Output\ DC\ power}{Input\ RF\ power} \times 100 \qquad (1)$$

For this circuit, the power conversion efficiency is found

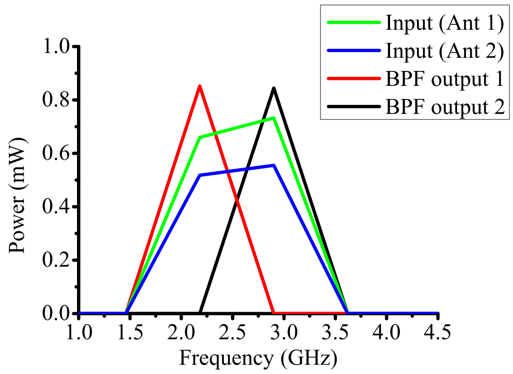

Figure 9. Power at the input of network and output of BPF.

to be 68.8 % corresponding to the input power of 5dBm as shown in Fig. 10. The return loss at corresponding input power is found to be 17.6 dB.

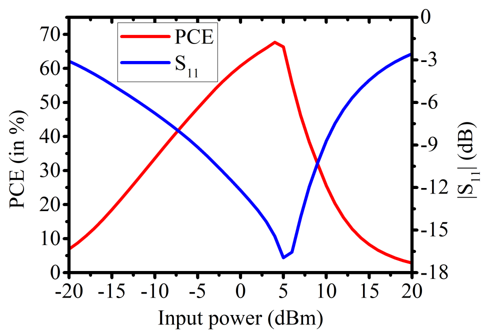

Figure 10. Power conversion efficiency and return loss plot for the rectifying circuit.

5 Conclusion

A dual band dual polarized antenna working at frequencies of 2.2 GHz and 2.9 GHz has been integrated with a energy harvesting through a network consisting of a rat race coupler and a dual frequency wilkinson power divider. The harvesting circuit at 4 dBm input power provides a power conversion efficiency of 68.8 %. The advantage of the proposed antenna is that it simultaneously transmit and as well as harvest energy from the GSM band with polarization flexibility.

References

[1] Alu, A., Engheta, N., Erentok, A., and Ziolkowski, R. W. (2007), "Single-Negative, Double-Negative, and Low-index Metamaterials and their Electromagnetic Applications", *IEEE Antennas and Propagation Magazine*, **49**, 1, pp. 23–36, doi:10.1109/MAP.2007.370979

[2] Kandasamy, K., Majumder, B., Mukherjee, J., and Ray, K. P. (2015), "Low-RCS and Polarization-Reconfigurable Antenna Using Cross-Slot-Based Metasurface," *IEEE Antennas and Wireless Propagation Letters*, **14**, pp. 1638–1641, doi: 10.1109/LAWP.2015.2415585

[3] Majumder, B., Krishnamoorthy, K., Mukherjee, J., and Ray, K. P. (2016), "Compact Broadband Directive Slot Antenna Loaded With Cavities and Single and Double Layers of Metasurfaces," *IEEE Transactions on Antennas and Propagation*, **64**, 11, pp. 4595–4606, doi: 10.1109/TAP.2016.2601346

[4] Majumder, B., Krishnamoorthy, K., Mukherjee, J., and Ray, K. P. (2016), "Frequency-Reconfigurable Slot Antenna Enabled by Thin Anisotropic Double Layer Metasurfaces," *IEEE Transactions on Antennas and Propagation*, **64**, 4, pp. 1218–1225, doi: 10.1109/TAP.2016.2526081

[5] Nasser, S. S. S., Liu, W., and Chen, Z. N. (2018). "Wide Bandwidth and Enhanced Gain of a Low-Profile Dipole Antenna Achieved by Integrated Suspended Metasurface", *IEEE Transactions on Antennas and Propagation*, **66**, 3, pp. 1540–1544, doi:10.1109/TAP.2018.2790161

[6] Sun, H., Guo, Y., He, M., and Zhong, Z. (2013), "A Dual-Band Rectenna Using Broadband Yagi Antenna Array for Ambient RF Power Harvesting", *IEEE Antennas and Wireless Propagation Letters*, **12**, pp. 918–921. doi:10.1109/LAWP.2013.2272873.

[7] Tran, L.-G., Cha, H.-K., and Park, W.-T. (2017), "RF power harvesting: a review on designing methodologies and applications", *Micro and Nano Systems Letters*, **5**, 1, 14, doi:10.1186/s40486-017-0051-0.

[8] Mavaddat, A., Armaki, S. H. M.,and Erfanian, A. R. (2015), "Millimeter-Wave Energy Harvesting Using 4x4 Microstrip Patch Antenna Array", *IEEE Antennas and Wireless Propagation Letters*, **14**, pp. 515–518, doi:10.1109/LAWP.2014.2370103.

[9] Yang, X.-X., Jiang, C., Elsherbeni, A. Z., Yang, F., and Wang, Y.-Q. (2013), "A Novel Compact Printed Rectenna for Data Communication Systems", *IEEE Transactions on Antennas and Propagation*, **61**, 5, pp. 2532–2539, doi:10.1109/TAP.2013.2244550.

[10] D. M. Pozar, Microwave Engineering, Wiley, 2004.

[11] Wu, L., Sun, Z., Yilmaz, H., and Berroth, M. (2006), "A dual-frequency wilkinson power divider", *IEEE Transactions on Microwave Theory and Techniques*, **54**, 1, pp. 278–284, doi: 10.1109/TMTT.2005.860300.

[12] Keysight Advanced Design System v.01 [Computer software] (2017).

[13] "HSMS-285x Series Surface Mount Microwave Schottky Detector Diodes," 2009.

[14] CST-Microwave Studio [Computer software] (2018).